Optica Applicata, Vol. XXXVII, No. 3, 2007

Scalar and vectorial approaches to cavity modes of the GaAs-based 1.3-μm oxide-confined edge emitting diode laser

TOMASZ CZYSZANOWSKI[1, 2*], WŁODZIMIERZ NAKWASKI[1]

[1]Laboratory of Computer Physics, Institute of Physics, Technical University of Łódź, ul. Wólczańska 219, 90-924 Łódź, Poland

[2]CFD Research Corporation, 215 Wynn Drive, Huntsville, Alabama 35805, USA

*Corresponding author: czyszan@p.lodz.pl

The modelling of optical fields within cavities of GaAs-based oxide-confined edge-emitting diode lasers is analysed treating the 1.3-μm InGaAs/GaAs quantum-well laser as an example of a typical device. Usability of two different optical approaches is compared. While in the first approach, based on the scalar wave simplification, optical fields within laser resonators are found to be composed of the TE modes, an alternative, more precise vectorial approach leads to the hybrid modes: EH and HE. Advantages and disadvantages of both methods are discussed and their validity limits in determination of mode intensities are compared. Simplified scalar approaches have often happened to be surprisingly exact, except for their weaker guidance occurring for higher-order modes, narrower aperture widths and/or thinner oxidation layers, when more exact but also more time-consuming vectorial approaches should be exclusively used.

Keywords: laser simulations, laser modes, edge emitting diode lasers.

1. Introduction

Recently, resonators of semiconductor lasers have often been reduced to relatively small dimensions to enable reduction of both their threshold currents and an increase in operation temperature. To design such lasers ensuring even better performance, an exact simulation of simultaneous interrelations between electrical, thermal, gain, stress and optical phenomena taking place within the device volumes when in operation is essential.

The modelling of optical field appears to be a very challenging problem since Maxwell's equations, treated rigorously, are not separable within the semiconductor laser domain. Moreover, wavelengths of the propagating light within modern

structures become often comparable with their sizes, which makes the common use of plane waves in scalar optical models unjustified. In such a situation, it seems necessary to employ the full vectorial theoretical model describing optical phenomena, instead of its simplified scalar approach. However, the computational experiment shows that, suprisingly, the scalar approach gives sometimes quite satisfactory results even beyond limits of its confirmed validity, *e.g.*, in some modern micro-cavity devices. Therefore, it is necessary to examine the performance of both optical models when these are used to simulate an operation of specified laser devices to determine cases where less time-consuming and simpler scalar approaches may be used. In the present work, a comparison is made of the scalar and vectorial models represented by the effective index method and the method of lines, respectively, applied to the optical simulation of standard GaAs-based oxide-confined edge emitting diode lasers.

2. The scalar approach – the effective index method

The effective index method is the most commonly used scalar approach to the optical phenomena within semiconductor lasers [1–4]. The model assumes that changes of the refractive index are relatively small and the propagating wave is the plane one. Therefore, the electromagnetic wave may be treated as a scalar field, which may be separated into independent functions describing the electromagnetic wave separately along each direction.

Let us assume here that the z-axis of the Cartesian coordinate system is parallel to the direction of wave propagation and the p-n junction of the structure lies in the x–z plane where $x = 0$ corresponds to the active-region centre (Fig. 1). Taking advantage of the concept of the effective refractive index as well as making use of the assumptions that the wave propagates within the charge-free medium and the time dependence of the solution has a form of the function of type $\exp(i\omega t)$, the set of Maxwell's equations may be reduced to the Helmholtz equation [5]:

$$\partial_x^2 \mathbf{E} + \partial_y^2 \mathbf{E} + k_0^2 \left[n^2(x, y) - N_{\text{eff}}^2 \right] \mathbf{E} = 0 \tag{1}$$

where $\partial_u \equiv \partial/\partial u$, $u = x, y$, $\mathbf{E}$ is the electric field vector of the electromagnetic wave, n – the position dependent complex refractive index of the laser domain, k_0 – the vacuum wave number, and N_{eff} – the structure complex effective index. The field distribution within the domain of the waveguide is assumed to be a product of two functions, which is true only for a uniform, free source domain:

$$E(x, y) = E_x(x) E_{xy}(x, y) \tag{2}$$

The function $E_x(x)$ is expected to approach precisely the solution in the x-direction, whereas the second one, $E_{xy}(x, y)$, is only weakly x-dependent. After some manipulations, one can get two plane wave equations:

$$\partial_y^2 E_{xy} + k_0^2\left[n^2(x,y) - n_i^2(y)\right]E_{xy} = 0 \tag{3}$$

$$\partial_x^2 E_x + k_0^2\left[n_i^2(y) - N_{\text{eff}}^2\right]E_x = 0 \tag{4}$$

where n_i denotes the complex effective index for the region assumed to be uniform in the x-direction. From equation (3), one can find the effective index n_i for each region, next setting n_i to equation (4), one can find the structure effective index N_{eff} for the whole structure. The general solution of the wave equations (3) and (4) for the uniform region may be expressed as a superposition of two waves travelling in the opposite directions:

$$E(u) = A\exp\left[\gamma(u-u_j)\right] + B\exp\left[-\gamma(u-u_j)\right] \tag{5}$$

where $u = x, y$, and $\gamma \equiv k_0\sqrt{n_e^2 - n_m^2}$ (n_e and n_m for Eq. (3) are n and n_i, respectively, and for Eq. (4) – n_i and N_{eff}, respectively), u_j stands for the position of the edge of the region. The regions are assumed to be rectangularly shaped. Amplitudes A and B and parameter γ can be found using the transfer matrix method [6].

3. The vectorial approach – the method of lines

Hitherto known vectorial models used to simulate optical fields in diode lasers are relatively complex and they often need special very time-consuming calculation algorithms. To this end, a more efficient new vectorial approach, namely the method of lines, was developed by R. Pregla and his group [7].

The initial set of Maxwell's equations is expressed in the form given, for example, by SALEH and TEICH [5]. Assuming oscillating dependence on time and on direction of propagation of both the electric field and magnetic field vectors, one can get the following set:

$$\partial_y \overline{\mathbf{E}} = -i\eta_0 \begin{bmatrix} k_0\left(1 - \dfrac{N_{\text{eff}}^2}{n^2}\right) & \dfrac{iN_{\text{eff}}}{n^2}\partial_x \\ iN_{\text{eff}}\partial_x\dfrac{1}{n^2} & \dfrac{1}{k_0}\partial_x\dfrac{1}{n^2}\partial_x + k_0 \end{bmatrix} \overline{\mathbf{H}} \equiv -i\eta_0 \mathbf{R}_{\mathbf{H}}\overline{\mathbf{H}} \tag{6}$$

$$\partial_y \overline{\mathbf{H}} = -\frac{i}{\eta_0}\begin{bmatrix} \dfrac{1}{k_0}\partial_x^2 + k_0 n^2 & -iN_{\text{eff}}\partial_x \\ -iN_{\text{eff}}\partial_x & k_0\left(n^2 - N_{\text{eff}}^2\right) \end{bmatrix} \overline{\mathbf{E}} \equiv -\frac{i}{\eta_0}\mathbf{R}_{\mathbf{E}}\overline{\mathbf{E}} \tag{7}$$

where, for simplicity, we take:

$$n \equiv n(x, y), \qquad \overline{\mathbf{E}} = \begin{bmatrix} E_z \\ -E_x \end{bmatrix}, \qquad \overline{\mathbf{H}} = \begin{bmatrix} H_x \\ H_z \end{bmatrix}, \qquad \eta_0 = \sqrt{\frac{\mu_0}{\varepsilon_0}}$$

A combination of the two above equations results in:

$$\partial_y^2 \overline{\mathbf{E}} = -\mathbf{R_H R_E} \overline{\mathbf{E}} \equiv -\mathbf{Q}_\mathbf{E}^2 \overline{\mathbf{E}} \tag{8}$$

After discretisation of Eq. (8) in the x-direction [7], it can be solved by diagonizing the matrix $\mathbf{Q_E}$. This enables us to find a characteristic value of the problem, which corresponds to the effective index value, as well as characteristic vectors which determine the distribution of the electromagnetic field within the structure. For Eq. (8) rewritten in the new base:

$$\partial_y^2 \hat{\mathbf{E}} + \Gamma_\mathbf{E}^2 \hat{\mathbf{E}} = 0 \tag{9}$$

where $\hat{\mathbf{E}} \equiv \mathbf{T}_\mathbf{E}^{-1} \overline{\mathbf{E}}$, the matrix $\mathbf{T_E}$ diagonizes $\mathbf{Q_E}$. The solution to Eq. (9) has the form of a standing wave:

$$\hat{\mathbf{E}}(y) = \mathbf{A}\cosh(i\Gamma_\mathbf{E} y) + \mathbf{B}\sinh(i\Gamma_\mathbf{E} y) \tag{10}$$

Some algebraic manipulations lead to the relation between the electric and the magnetic fields within the layer assumed to be uniform in the y-direction:

$$\begin{bmatrix} \hat{\mathbf{H}}_\mathbf{0}^{(i)} \\ -\hat{\mathbf{H}}_\mathbf{d}^{(i)} \end{bmatrix} = \begin{bmatrix} \mathbf{y}_\mathbf{1}^{(i)} & \mathbf{y}_\mathbf{2}^{(i)} \\ \mathbf{y}_\mathbf{2}^{(i)} & \mathbf{y}_\mathbf{1}^{(i)} \end{bmatrix} \begin{bmatrix} \hat{\mathbf{E}}_\mathbf{0}^{(i)} \\ \hat{\mathbf{E}}_\mathbf{d}^{(i)} \end{bmatrix} \tag{11}$$

where $\hat{\mathbf{H}}$ is the vector of the magnetic field components transformed to the base in which the matrix $\mathbf{Q_E}$ can be diagonized. The superscript indicates the number of the layer, and the subscript the edge of the same layer; $\mathbf{y_1}$ and $\mathbf{y_2}$ are defined as follows:

$$\mathbf{y_1} = \left(\mathbf{T}_\mathbf{E}^{-1}\mathbf{R_H T_H}\right)^{-1} \Gamma_\mathbf{E} \tanh^{-1}(i\Gamma_\mathbf{E} d) \tag{12}$$

$$\mathbf{y_2} = -\left(\mathbf{T}_\mathbf{E}^{-1}\mathbf{R_H T_H}\right)^{-1} \Gamma_\mathbf{E} \sinh^{-1}(i\Gamma_\mathbf{E} d) \tag{13}$$

From Eq. (11) one can find the relation between the magnetic and the electric fields:

$$\hat{\mathbf{H}}_\mathbf{d}^{(i)} = \mathbf{Y}^{(i)} \hat{\mathbf{E}}_\mathbf{d}^{(i)} \tag{14}$$

where

$$\mathbf{Y}^{(i)} = -\left\{\mathbf{y}_2^{(i)}\left[\left(\mathbf{T}_\mathbf{H}^{(i)}\right)^{-1}\mathbf{T}_\mathbf{H}^{(i-1)}\mathbf{Y}^{(i-1)}\left((\mathbf{T}_\mathbf{E}^{(i)})^{-1}\mathbf{T}_\mathbf{E}^{(i-1)}\right)^{-1} - \mathbf{y}_1^{(i)}\right]^{-1}\mathbf{y}_2^{(i)} + \mathbf{y}_1^{(i)}\right\} \tag{15}$$

The assumption of the electric field decaying on the borders of the simulated domain yields the eigenvalue equation for the vector of the electric field between arbitrarily chosen layers m and l:

$$\left[\mathbf{T}_\mathbf{H}^{(m)}\mathbf{Y}^{(m)}\left(\mathbf{T}_\mathbf{E}^{(m)}\right)^{-1} - \mathbf{T}_\mathbf{H}^{(l)}\mathbf{Y}^{(l)}\left(\mathbf{T}_\mathbf{E}^{(l)}\right)^{-1}\right]\bar{\mathbf{E}} = \mathbf{M}\bar{\mathbf{E}} = 0 \tag{16}$$

The solution of the above equation determines the characteristic values which correspond to the complex effective refractive index N_{eff} and eigenvectors related to the electric field. The equation is not trivial only if **M** is singular, then at least one eigenvalue of **M** is equal to zero.

4. The results

Usually, in the simulation of a laser operation, the final task is to calculate its output power as a function of applied voltage (or supply current). This makes it necessary to model self-consistently a complex network of interrelations between electrical, thermal, gain and optical phenomena. All they interact with the optical model influencing both (real and imaginary) parts of the complex refractive indices of structure layers. But the focus of this paper is on purely optical determination of the optical modes with the help of both scalar and vectorial approaches. Taking additionally into account an impact of gain, thermal and electrical phenomena on optical ones, can make it difficult to unambiguously interpret the results of analysis. On the other hand, a purely optical comparison of scalar and vectorial modes may enable determination of their validity limits, which is the main goal of this paper. Therefore, details of recombination processes, carrier transport and thermal flow are intentionally omitted here by using a constant optical gain (a step-like gain distribution) within the active quantum wells (QW's) of the structure. Our goal is to calculate the cavity modes using both approaches and to compare their distributions.

Let us consider a standard design of the highly strained, stripe-geometry 1.3-μm InGaAs/GaAs double quantum well edge emitting (Fabry–Perot) diode laser [8]. Its layer structure is shown in Fig. 1 and details are listed in the Table. Its active region consists of two strained $In_{0.44}Ga_{0.56}As$ quantum wells separated with the GaAs barrier. The necessary lateral confinement of the current flow and the optical field is realized with the aid of a 0.15 μm oxidized layer.

The scalar modes are assumed to be polarized (TE polarization) whereas the vectorial modes have been found to be hybrid ones. This means that the vectorial modes are determined by all six components of the electromagnetic field contrary to the scalar

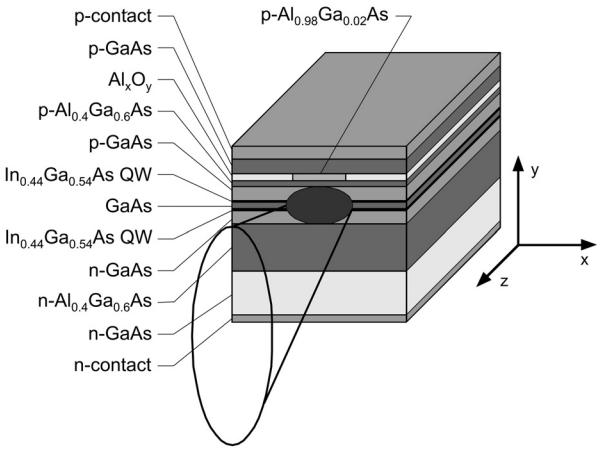

Fig. 1. A schematic structure of the edge-emitting diode laser and the coordinate system applied in the analysis.

modes, which are defined by three components only. Figure 2 presents intensity profiles of three lowest-order modes for the laser structure with a 12-μm stripe width. One can observe a distinctly better confinement of the fundamental vectorial mode within the active region than its scalar counterpart (Fig. 2**a**). It becomes even more pronounced for higher order modes, especially in the *x*-direction. Distinct leakage of scalar modes brings out the lowering of the real and imaginary parts of the mode effective refractive index since their electromagnetic fields penetrate the lateral passive regions exhibiting lower index and high absorption. On the other hand, vectorial modes suffer from the diffraction losses, which are not included in the scalar approach.

T a b l e. Construction details of the highly strained, double quantum-well edge-emitting diode laser [8]. The gain within the active region corresponds to the carrier concentration equal to 3×10^{18} cm^{-3}. The values of refractive indices and gain coefficients have been taken from [9, 10].

Material	Thickness [nm]	Doping concentration [cm^{-3}]	Real refractive index	Optical gain coefficient [cm^{-1}]
p-GaAs	500	10^{19}	3.453	–226.379
$p\text{-}Al_{0.98}Ga_{0.02}As/Al_2O_3$	150	10^{19}	3.453/1.75	–226.379/0
$p\text{-}Al_{0.4}Ga_{0.6}As$	300	4×10^{17}	3.239	–64.9326
p-GaAs	100	10^{16}	3.481	–58.374
$In_{0.44}Ga_{0.56}As$	7	0	3.533	1171.78
GaAs	20	0	3.482	0
$In_{0.44}Ga_{0.56}As$	7	0	3.533	1171.78
n-GaAs	100	5×10^{16}	3.481	–59.0466
$n\text{-}Al_{0.4}Ga_{0.6}As$	1500	10^{18}	3.237	–75.0228
n-GaAs	5000	10^{18}	3.478	–75.0228
			Emitted wavelength	1.23 μm

Next important difference, which is more pronounced for higher order modes, is connected with different values of intensity maxima within the active region. For a uniform region, the scalar solution is given by the sum of exponential functions, as

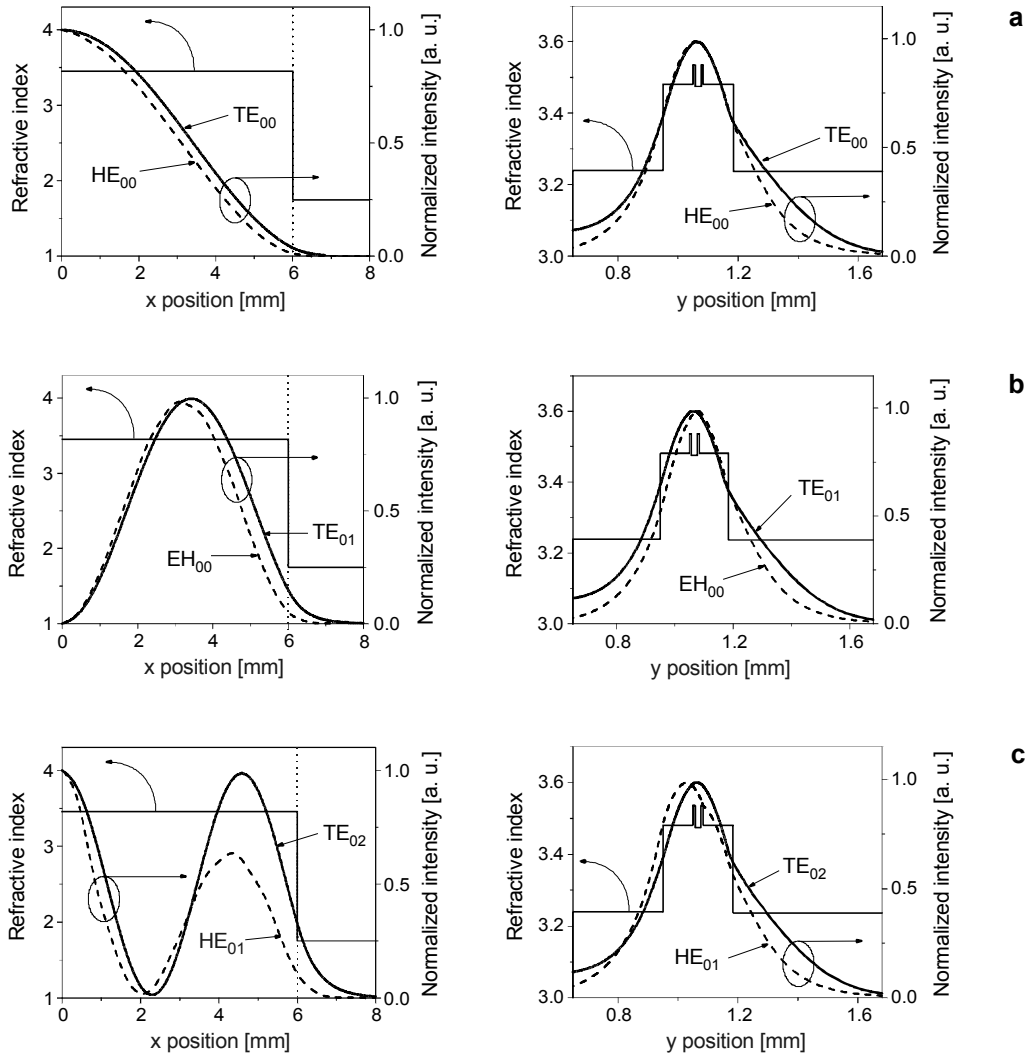

Fig. 2. Intensity profiles of the three lowest order modes calculated with the scalar (solid lines) and the vectorial (dashed lines) approaches for the highly strained 1.3-μm InGaAs/GaAs double quantum-well edge-emitting (Fabry–Perot) diode laser [8], with the stripe active region defined by a 12 μm aperture width. The left column of the figures depicts profiles of the mode intensities along the *x*-direction within the active region, whereas the right one presents the analogous profiles along the *y*-axis on the symmetry plane. The figures correspond to: HE_{00} and TE_{00} modes (**a**), EH_{00} and TE_{01} modes (**b**), HE_{01} and TE_{02} modes (**c**). Profiles of the refractive index along the *x*- (within oxide layer) and the *y*-axis are additionally shown.

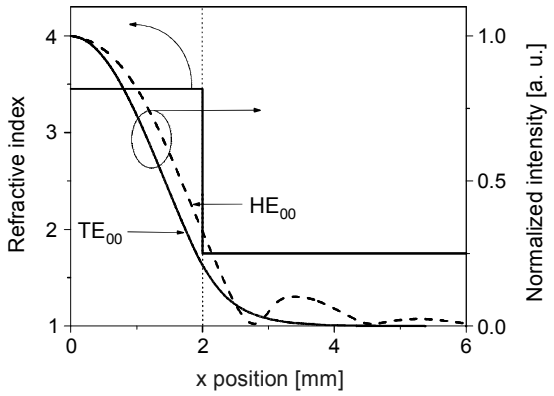

Fig. 3. Profiles of the fundamental mode intensity along *x*-axis calculated with the aid of the scalar (solid lines) and the vectorial (dashed lines) approaches for the diode-laser structure [8] defined by a 4 μm aperture width. Profile of the refractive index along *x*-axis within the oxide layer is additionally shown.

if the region were infinite. Hence, the intensity oscillations of scalar modes exhibit a constant amplitude (*cf*. Fig. 2**c**). Besides the differences in the intensity distributions of the modes in the *y*-direction express the essential difference between the models. The scalar approach separates the solution for *x*- and *y*-directions. Hence, the mode intensity profile in the *y*-direction remains completely independent of the *x*-directional solution. The non-separated solution of the vectorial approach predicts the shift of the higher-order modes towards the *p*-contact (Fig. 2**c**), since those modes are weaker confined by the oxidation, and finally the high refractive index of the broad *p*-contact layer may even attract the modes, as considered below.

Figure 3 presents the difference in the mode intensity profile along the *x*-direction between the results of the scalar and the vectorial optical models for a narrow stripe width of 4 μm. Compared to Fig. 2**a**, the narrowing of the oxide window causes a more pronounced penetration by the mode of the lateral passive regions placed out of the central active region. This finally leads to the mode leakage. Both approaches predict such a behaviour, however, vectorial model indicates the diffraction process as the main reason for the leakage. The vectorial mode penetrating the regions out of the active region starts to oscillate (Fig. 3), which reduces the guiding process enhanced by the oxidations. The scalar model predicts considerably less pronounced penetration of the lateral passive region out of the active region by the mode without appearance of any oscillations caused by the diffraction.

Figure 4 presents an interesting process of weak guidance. Two structures with the oxidation layer of different thicknesses are considered. Thick oxidation ensures a stable waveguide process, whereas thin one allows the wave leaking. This time the leakage occurs in the *y*-direction. As one can see, too thin an oxidation layer does

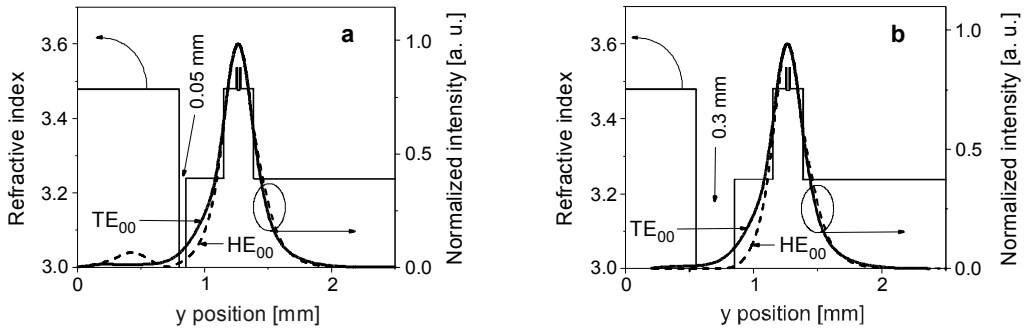

Fig. 4. Profiles of the fundamental mode intensity along *y*-axis calculated with the aid of the scalar (solid lines) and the vectorial (dashed lines) approaches for the structure [8] defined by a 12 μm aperture width in the oxide layer of 0.05 μm (**a**) and 0.3 μm (**b**) thickness. Profile of the refractive index along the *y*-axis is additionally shown.

not protect a mode optical field from its migration towards the high refractive *p*-contact layer. For a narrower oxidation layer, the vectorial model reveals an essential mode leakage and its oscillations within the *p*-contact layer whereas the scalar one penetrates this layer without any oscillations. This means that too narrow an oxidation layer may lead to a considerable increase in optical losses, which is followed by an increase in a lasing threshold.

5. Conclusions

Two approaches intended for simulation of the electromagnetic field within the cavity of edge emitting (Fabry–Perot) diode lasers are presented. The less exact scalar approach owes its extremely short calculation time to the plane wave assumption. On the other hand, the vectorial models, of which the method of lines is currently the most effective one, need usually 10^2–10^3 times longer calculation time. The comparison of the mode profiles determined using both approaches reveals a better confinement of vectorial modes within the active region. This is a consequence of the assumed plane wave solution used in simplified scalar approaches which has been taken from the infinite domain and set to the finite region. Nevertheless, profiles of the modes determined using both approaches are usually surprisingly close, except for the weaker guidance occurring for higher-order modes, narrower aperture widths and/or thinner oxidation layers. The above restrictions define validity limits of simple scalar optical approaches in modelling optical fields within cavities of standard edge-emitting diode lasers.

Acknowledgements – This work was supported by the Stipend for Young Scientists from the Foundation for Polish Science and by the Polish Ministry of Science and Information Society Technologies (MNiI), grant No. 3-T11B-073-29.

References

[1] BERGMANN M.J., CASEY H.C. JR., *Optical-field calculations for lossy multiple-layer $Al_xGa_{1-x}N/In_xGa_{1-x}N$ laser diodes*, Journal of Applied Physics **84**(3), 1998, pp. 1196–203.

[2] MARRIS D., CORDAT A., PASCAL D., KOSTER A., CASSAN E., VIVIEN L., LAVAL S., *Design of a SiGe-Si quantum-well optical modulator*, IEEE Journal of Selected Topics in Quantum Electronics **9**(3), 2003, pp. 747–54.

[3] SERRAT C., VAN EXTER M.P., VAN DRUTEN N.J., WOERDMAN J.P., *Transverse mode formation in microlasers by combined gain- and index-guiding*, IEEE Journal of Quantum Electronics **35**(9), 1999, pp. 1314–21.

[4] CZYSZANOWSKI T., NAKWASKI W., *Mode transformation enhanced in nitride diode lasers by modification of their buffer layers*, Journal of Physics D: Applied Physics **34**(9), 2001, pp. 1277–85.

[5] SALEH B.E.A., TEICH M.C., *Fundamentals of Photonics*, John Wiley & Sons, New York 1991.

[6] CZYSZANOWSKI T., WASIAK M., NAKWASKI W., *Design considerations for GaAs/(AlGa)As SCH and GRIN-SCH quantum-well laser structures. I. The model*, Optica Applicata **31**(2), 2001, pp. 313–23.

[7] ROGGE U., *Method of Lines for the Analysis of Dielectric Waveguides*, PhD Thesis, Fern Universitat, Hagen 1991.

[8] KONDO T., ARAI M., ONOMURA A., MIYAMOTO T., KOYAMA F., *1.23 μm long wavelength highly strained GaInAs/GaAs quantum well laser*, 15th Annual Meeting of the IEEE Lasers and Electro-Optics Society, Vol. 2, p. 618.

[9] JENKINS D.W., *Optical constants of $Al_xGa_{1-x}As$*, Journal of Applied Physics **68**(4), 1990, pp. 1848–53.

[10] ADACHI S., *Physical Properties of III-V Semiconductor Compounds*, John Wiley & Sons, New York 1992.

Received July 10, 2006